

## Sonochemistry of Alcohol-Water Mixtures: Spin-Trapping Evidence for Thermal Decomposition and Isotope-Exchange Reactions

C. Murali Krishna, Takashi Kondo,<sup>†</sup> and Peter Riesz\*

Radiation Oncology Branch, Clinical Oncology Program, Division of Cancer Treatment, National Cancer Institute, National Institutes of Health, Bethesda, Maryland 20892 (Received: November 23, 1988)

The sonochemistry of argon-saturated water-alcohol mixtures has been studied by ESR and spin trapping with 3,5-dibromo-4-nitrosobenzenesulfonate. Free-radical intermediates induced by 50-kHz ultrasound in aqueous solutions of ethanol, 1-propanol, 2-propanol, and 2-methyl-2-propanol were identified. Spin adducts typical of thermal decomposition of the alcohols and of H- and OH-induced abstraction reactions were observed. In the sonolysis of mixed-isotope systems of the type ROD-D<sub>2</sub>O and CH<sub>3</sub>CD<sub>2</sub>OH-H<sub>2</sub>O, isotopically mixed radicals were spin trapped, indicating the occurrence of multiple radical recombination reactions in the gas phase of the collapsing gas bubbles. The spin adduct yields of methyl radicals and of  $\dot{\text{C}}\text{H}_2\text{CH}_2\text{OH}$  radicals obtained by sonolysis of water-ethanol mixtures were studied over a wide range of solvent composition, and two maxima were observed for both species. The first maximum occurs below 5 M ethanol and can be explained in terms of changes in spin-trapping efficiency due to competition between radical-spin trap and radical-ethanol reactions. The second maximum occurs at 10 M ethanol and is due to changes in acoustic cavitation. The effect of temperature on the sonochemical yield of 10% ethanol was studied and the yield was found to decrease with increasing temperature in the range 25-50 °C, indicating the predominant effect of vapor pressure of the bulk solvent on sonochemical yields.

### Introduction

Acoustic cavitation induces a wide variety of chemical reactions. The chemical, physical, and biological effects of ultrasound and its applications have recently been reviewed.<sup>1</sup> Aqueous sonochemistry has received much attention,<sup>2</sup> and the results are understood in terms of reactions occurring in three different regions of cavitating gas bubbles. The first region is the interior of the collapsing gas bubbles in which extreme conditions of temperature (several thousand kelvin) and pressure (several hundred atmospheres) exist transiently, which induce chemical reactions yielding products that are typical of pyrolysis reactions in the gas phase. In aqueous solutions, thermal decomposition of water leads to the formation of H and OH radicals.<sup>3</sup> A typical reaction in the gas phase is the isotopic exchange between deuterium and water vapor occurring during the sonolysis of D<sub>2</sub>-H<sub>2</sub>O mixtures.<sup>4</sup>

The second region of interest is the interfacial region between the collapsing gas bubbles and the bulk solvent where the temperatures are relatively lower than in the interior of the gas bubbles but high enough to induce free-radical reactions. The free radicals observed in this region originate from nonvolatile solutes that can accumulate in high enough concentrations to undergo thermal decomposition.<sup>5</sup> The relative efficiencies of solutes to undergo thermal decomposition in this region depend on their ability to accumulate in the gas-liquid interfacial region and on the activation energies for bond scission: the more the solute accumulates and the lower the activation energy, the higher the yield of thermal decomposition products. Recent observations suggest that for a given nonvolatile solute, at low concentrations, scavenging of H and OH radicals by the solute molecules occurs. At high concentrations, the products due to pyrolysis predominate.<sup>5</sup>

Finally, in the third region, namely the bulk solvent, the sonochemically induced free radicals produced in the interior of the gas bubbles and in the interfacial regions escape into the bulk of the liquid and undergo scavenging reactions with solutes present in the bulk liquid in a manner similar to those observed in aqueous radiation chemistry.<sup>6</sup>

Sonochemical studies in organic liquids reported by Suslick and his co-workers<sup>7</sup> demonstrate that organic liquids do support acoustic cavitation and the associated sonochemistry. Suslick et al.<sup>8</sup> have also experimentally determined the effective temperatures of the interior of the gas bubbles (5200 ± 650 K) and of the surrounding thin shell (1900 ± 200 K). More recently, direct observation of sonoluminescence from organic liquids has unambiguously proved the role of acoustic cavitation in the sonochemistry of organic liquids.<sup>9</sup>

The sonochemistry of water-alcohol mixtures is of interest because of the increasing use of ultrasound in organic synthesis.<sup>10</sup> We have found that 3,5-dibromo-4-nitrosobenzenesulfonate (DBNBS) is the spin trap of choice for aqueous sonolysis studies. The sulfonate group ensures nonvolatility, and several carbon-centered radical adducts show sufficiently detailed spectra to allow the identification of the trapped radical.<sup>11,12</sup> The sonochemistry of aqueous methanol has been reported with use of ESR and spin-trapping techniques.<sup>11</sup> Evidence for thermal decomposition of methanol giving rise to methyl radicals in water has been obtained. Also, isotopically labeled methyl radicals, CH<sub>2</sub>D and  $\dot{\text{C}}\text{H}\text{D}_2$ , were observed when CH<sub>3</sub>OD-D<sub>2</sub>O mixtures were sonicated. The radical yield has been studied as a function of the solvent composition and the various factors affecting the yields have been discussed.

In the present work, the sonochemistry of aqueous solutions of ethanol, 1-propanol, 2-propanol, and 2-methyl-2-propanol was studied in order to characterize the various pyrolytic and H- and OH-induced free radicals from these volatile solutes.

### Materials and Methods

**Chemicals.** D<sub>2</sub>O, ethanol, 1-propanol, 2-propanol, and 2-methyl-2-propanol were purchased from Aldrich. CH<sub>3</sub>CH<sub>2</sub>OD, CH<sub>3</sub>CD<sub>2</sub>OH, CD<sub>3</sub>CH<sub>2</sub>OH, CH<sub>3</sub><sup>13</sup>CH<sub>2</sub>OH were obtained from Merck, Sharpe, and Dohme. The sodium salt of 3,5-dibromo-

(1) Suslick, K. S. In *Ultrasound: Its Chemical, Physical and Biological Effects*; Suslick, K. S., Ed.; VCH: New York, 1988.

(2) (a) Elpiner, I. E. *Ultrasound, Physical Chemistry and Biological Effects*; Consultants Bureau: New York, 1964. (b) Henglein, A. *Ultrasonics* **1987**, *25*, 6.

(3) Makino, K.; Mossoba, M. M.; Riesz, P. *J. Phys. Chem.* **1983**, *87*, 1369.

(4) Fischer, Ch.-H.; Hart, E. J.; Henglein, A. *J. Phys. Chem.* **1986**, *90*, 222.

(5) (a) Gutierrez, M.; Henglein, A.; Fischer, Ch.-H. *Int. J. Radiat. Biol. Relat. Stud. Phys., Chem. Med.* **1986**, *50*, 313. (b) Kondo, T.; Murali Krishna, C.; Riesz, P. *Radiat. Res.*, in press.

(6) Kondo, T.; Murali Krishna, C.; Riesz, P. *Int. J. Radiat. Biol. Relat. Stud. Phys., Chem. Med.* **1988**, *53*, 891.

(7) (a) Suslick, K. S.; Schubert, P. F.; Goodale, J. W. *Ultrason. Symp. Proc.* **1981**, *2*, 612. (b) Suslick, K. S.; Gawienowski, J. J.; Schubert, P. F.; Wang, H. H. *J. Phys. Chem.* **1983**, *87*, 2299.

(8) Suslick, K. S.; Hammerton, D. A.; Cline, R. E., Jr. *J. Am. Chem. Soc.* **1986**, *108*, 5641.

(9) Suslick, K. S.; Flint, E. B. *Nature* **1987**, *330*, 553.

(10) Suslick, K. S. In *Modern Synthetic Methods*; Scheffold, R., Ed.; Springer-Verlag: New York, 1986; Vol. 4.

(11) Murali Krishna, C.; Lion, Y.; Kondo, T.; Riesz, P. *J. Phys. Chem.* **1987**, *91*, 5847.

(12) (a) Kaur, H.; Leung, K. H. W.; Perkins, M. J. *J. Chem. Soc., Chem. Commun.* **1982**, 142. (b) Ozawa, T.; Hanaki, A. *Bull. Chem. Soc. Jpn.* **1987**, *60*, 2304. (c) Smith, P.; Robertson, J. S. *Can. J. Chem.* **1988**, *66*, 1153.

<sup>†</sup> Permanent address: Department of Experimental Radiology and Health Physics, Fukui Medical School, Matsuoka, Fukui 910-11, Japan.



**TABLE I: Hyperfine Coupling Constants of DBNBS Adducts Obtained by Sonolysis and H<sub>2</sub>O<sub>2</sub>-UV Photolysis of Aqueous Alcohols and by Other Methods**

system	method	hyperfine coupling constants <sup>a</sup>			radical adduct
		a <sub>N</sub> , G	a <sub>H</sub> , G	a <sub>γH</sub> , G	
Ethanol					
CH <sub>3</sub> CH <sub>2</sub> OH-H <sub>2</sub> O (5%)	H <sub>2</sub> O <sub>2</sub> -UV	14.15	11.38 (2)		ĊH <sub>2</sub> CH <sub>2</sub> OH
CH <sub>3</sub> CH <sub>2</sub> OH-H <sub>2</sub> O (5%)	US	(a) 14.50	13.50 (3)		ĊH <sub>3</sub>
		(b) 14.15	11.38 (2)		ĊH <sub>2</sub> CH <sub>2</sub> OH
		(c) 13.50	8.95 (2)	0.50	ĊH <sub>2</sub> CHO
		(d) <sup>b</sup> 14.50	13.00 (2)		ĊH <sub>2</sub> ĊH <sub>2</sub>
CH <sub>3</sub> CHO-H <sub>2</sub> O (5%)	H <sub>2</sub> O <sub>2</sub> -UV	13.50	8.95 (2)	0.50	ĊH <sub>2</sub> CHO
CH <sub>3</sub> CH <sub>2</sub> I (1%) in CH <sub>3</sub> CH <sub>2</sub> OH-H <sub>2</sub> O (4%)	255 nm	14.50	13.00 (2)		ĊH <sub>2</sub> ĊH <sub>2</sub>
1-Propanol					
CH <sub>3</sub> (CH <sub>2</sub> ) <sub>2</sub> OH-H <sub>2</sub> O (5%)	H <sub>2</sub> O <sub>2</sub> -UV	(a) 14.38	12.25 (2)		ĊH <sub>2</sub> (CH <sub>2</sub> ) <sub>2</sub> OH
		(b) 14.00	8.00 (1)		ĊH <sub>2</sub> CHCH <sub>2</sub> OH or CH <sub>3</sub> CH <sub>2</sub> ĊHOH
CH <sub>3</sub> (CH <sub>2</sub> ) <sub>2</sub> OH-H <sub>2</sub> O (5%)	US	(a) 14.50	13.50 (3)		ĊH <sub>3</sub>
		(b) 14.00	8.00 (1)		ĊH <sub>2</sub> CHCH <sub>2</sub> OH or CH <sub>3</sub> CH <sub>2</sub> ĊHOH
		(c) 14.38	12.25 (2)		ĊH <sub>2</sub> (CH <sub>2</sub> ) <sub>2</sub> OH
		(d) <sup>b</sup> 14.00	6.25 (1)		not identified
2-Propanol					
(CH <sub>3</sub> ) <sub>2</sub> CHOH-H <sub>2</sub> O (5%)	H <sub>2</sub> O <sub>2</sub> -UV	14.00	11.50 (1); 9.60 (1')	0.50	CH <sub>3</sub> CHOHĊH <sub>2</sub>
(CH <sub>3</sub> ) <sub>2</sub> CHOH-H <sub>2</sub> O (5%)	US	(a) 14.50	13.50 (3)		ĊH <sub>3</sub>
		(b) 14.00	11.50 (1); 9.60 (1')	0.50	CH <sub>3</sub> CHOHĊH <sub>2</sub>
		(c) 13.50	9.25 (2)		ĊH <sub>2</sub> COCH <sub>3</sub>
(CH <sub>3</sub> ) <sub>2</sub> CO-H <sub>2</sub> O (5%)	H <sub>2</sub> O <sub>2</sub> -UV	13.50	9.25 (2)		ĊH <sub>2</sub> COCH <sub>3</sub>
2-Methyl-2-propanol					
(CH <sub>3</sub> ) <sub>3</sub> COH-H <sub>2</sub> O (1%)	H <sub>2</sub> O <sub>2</sub> -UV	13.50	9.60 (2)		(ĊH <sub>2</sub> )(CH <sub>3</sub> ) <sub>2</sub> COH
(CH <sub>3</sub> ) <sub>3</sub> COH-H <sub>2</sub> O (1%)	US	(a) 14.50	13.50 (2)		ĊH <sub>3</sub>
		(b) 13.50	9.60 (2)		(ĊH <sub>2</sub> )(CH <sub>3</sub> ) <sub>2</sub> COH
		(c) 13.00	-		Ċ(CH <sub>3</sub> ) <sub>3</sub>

<sup>a</sup> The numbers in parentheses denote the number of equivalent protons in the spin adduct. <sup>b</sup> Hyperfine coupling constants for these spin adducts are approximate and indirectly obtained, as described in the text.

photolysis or  $\gamma$ -radiolysis experiments. In a recent report,<sup>12b</sup> in which OH radicals were generated by the Fe<sup>2+</sup>-H<sub>2</sub>O<sub>2</sub> (Fenton) system with ethanol as the substrate, the ĊH<sub>2</sub>CH<sub>2</sub>OH adduct DBNBS was observed, in agreement with our results. However, in a later report with the same Fenton reaction system and a rapid-flow system to generate OH radicals,<sup>12c</sup> CH<sub>3</sub>ĊHOH was trapped as the major species and ĊH<sub>2</sub>CH<sub>2</sub>OH was trapped in a smaller yield with DBNBS.

This difference in the experimental results was attributed to the differences in the steady-state reactant concentrations<sup>12c</sup> and also presumably due to the short half-life of the CH<sub>3</sub>ĊHOH adduct of DBNBS.

The ESR spectrum obtained by sonolysis of argon-saturated CH<sub>3</sub>CH<sub>2</sub>OH-H<sub>2</sub>O (5%) in the presence of DBNBS (3 mM) resulted in the observation of four different spin adducts (Figure 1b). The first spin adduct (lines marked A, Figure 1b) exhibited a primary nitrogen triplet ( $a_N = 14.5$  G), each line being further split into a 1:3:3:1 quartet due to three equivalent protons ( $a_{3H} = 13.5$  G). This ESR spectrum is characteristic of a ĊH<sub>3</sub> adduct of DBNBS.<sup>11,12</sup>

The second spin adduct (lines marked C, Figure 1b) obtained in the sonolysis of CH<sub>3</sub>CH<sub>2</sub>OH-H<sub>2</sub>O (5%) exhibited an ESR spectrum characteristic of a CH<sub>2</sub> radical ( $a_N = 14.15$  G;  $a_{2H} = 11.38$  G) and is consistent with the ĊH<sub>2</sub>CH<sub>2</sub>OH adduct of DBNBS since these splitting constants are identical with those observed for the ĊH<sub>2</sub>CH<sub>2</sub>OH adduct obtained in the H<sub>2</sub>O<sub>2</sub>-UV photolysis and the  $\gamma$ -radiolysis experiments. The assignment of this adduct has been confirmed by UV photolysis of ICH<sub>2</sub>CH<sub>2</sub>OH. When ICH<sub>2</sub>CH<sub>2</sub>OH-H<sub>2</sub>O (5%) was photolyzed with 255-nm light in the presence of DBNBS, a ĊH<sub>2</sub>CH<sub>2</sub>OH adduct of DBNBS was formed. The ESR parameters of this adduct were found to be identical with the spin adduct (lines marked C, Figure 1a) obtained by H<sub>2</sub>O<sub>2</sub>-UV photolysis of aqueous ethanol.

The ESR spectrum of the third spin adduct observed in the sonolysis of CH<sub>3</sub>CH<sub>2</sub>OH-H<sub>2</sub>O (5%) (lines marked B in Figure 1b,c) exhibits a primary nitrogen triplet ( $a_N = 13.5$  G), further split into a secondary 1:2:1 triplet ( $a_{2H} = 8.95$  G) due to two equivalent protons. Each of these secondary lines is further split into a doublet ( $a_{\gamma H} = 0.5$  G) by a proton at the  $\gamma$ -position (only

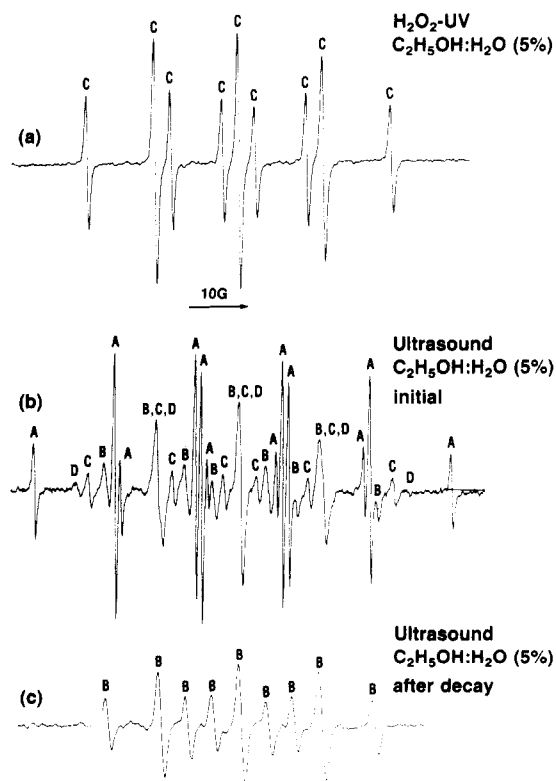


**Figure 1.** ESR spectra of spin adducts obtained from CH<sub>3</sub>CH<sub>2</sub>OH-H<sub>2</sub>O (5:95, v/v): (a) sample in the presence of H<sub>2</sub>O<sub>2</sub> (2 mM) and DBNBS (3 mM) after 2-min exposure to 275-nm light; (b) sonolysis (10 min) of argon-saturated solutions in the presence of DBNBS (3 mM), recorded immediately after sonication; (c) same conditions as (b), recorded 2 h after sonication.

observed under low microwave power and modulation amplitude), indicating that this spin adduct has been formed by addition of a radical of the type ĊH<sub>2</sub>CHX. The ESR spectrum of this spin

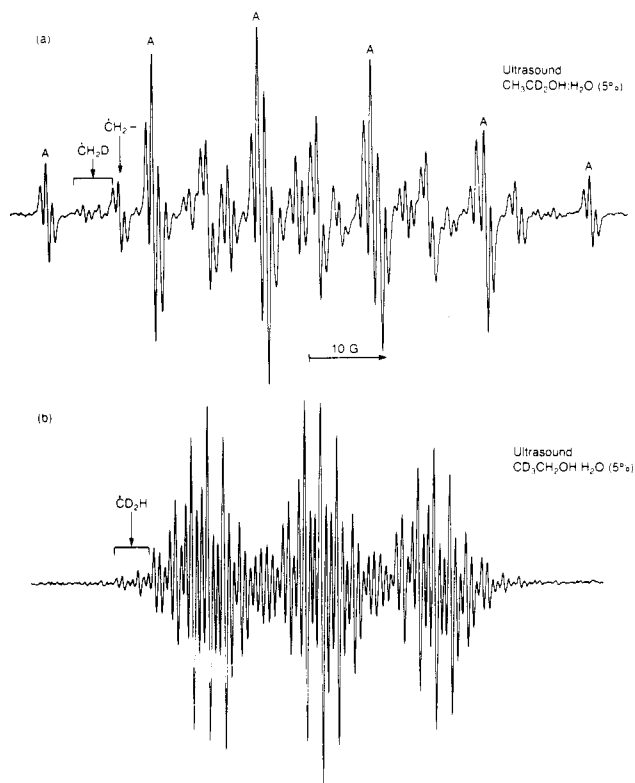


**Figure 2.** ESR spectra of spin adducts obtained by sonolysis (20 min) of argon-saturated ethanol–water mixture (5:95, v/v) in the presence of the nondeuterated form of DBNBS (10 mM): (a)  $\text{CH}_3\text{CD}_2\text{OH}-\text{H}_2\text{O}$  (5:95, v/v); (b)  $\text{CD}_3\text{CH}_2\text{OH}-\text{H}_2\text{O}$  (5:95, v/v).

adduct was found to be more stable than those of other spin adducts obtained by sonolysis of ethanol (Figure 1c). When the sonolysis experiment was repeated with  $\text{CH}_3\text{CD}_2\text{OH}$ , the  $\gamma$ -hydrogen splitting, which was observed for this spin adduct in the case of  $\text{CH}_3\text{CH}_2\text{OH}$ , was not observed. Gutierrez et al.,<sup>14</sup> in their study of the sonolysis of aqueous ethanol, reported the formation of acetaldehyde as one of the stable sonoproducts formed by disproportionation of two  $\text{CH}_3\dot{\text{C}}\text{HOH}$  radicals. Hence, the ESR spectrum of this adduct (lines marked B) could be due to the  $\text{CH}_2-\text{CH}=\text{O}$  radical. Additional support for this assignment has been obtained by the  $\text{H}_2\text{O}_2$ -UV photolysis experiments of  $\text{CH}_3\text{CHO}-\text{H}_2\text{O}$  (5%) in the presence of DBNBS (3 mM), in which the ESR spectrum was found to be identical with that obtained for the second spin adduct (lines marked B, Figure 1b).

Indications of a fourth spin adduct (lines marked D, Figure 1b) are found. However, this spin adduct was formed in relatively small quantities, and all the ESR lines corresponding to this adduct could not be located because of the overlap from the ESR lines of other spin adducts formed in larger quantities. However, the separation between the low-field and the high-field lines of this adduct could be measured and found to be 55 G, which is in the range expected for  $\dot{\text{C}}\text{H}_2-$  type adducts of DBNBS (45–55 G). Indirect support for the identification of this spin adduct has been obtained from the direct UV photolysis of  $\text{C}_2\text{H}_5\text{I}$ . When  $\text{C}_2\text{H}_5\text{I}$  (1%) in  $\text{C}_2\text{H}_5\text{OH}-\text{H}_2\text{O}$  (4%) was photolyzed at 255 nm in the presence of DBNBS, a  $\text{CH}_3\dot{\text{C}}\text{H}_2$  radical is formed, the DBNBS adduct of which exhibited a primary nitrogen triplet ( $a_{\text{N}} = 14.5$  G) and a secondary 1:2:1 triplet due to two equivalent protons ( $a_{2\text{H}} = 13.00$  G). The total spread of the spectrum has been measured to be 55 G. The total spread of a  $\dot{\text{C}}\text{H}_2-$  adduct of DBNBS is  $2(a_{\text{N}} + a_{2\text{H}})$ . The spread of the ESR spectrum of the  $\text{CH}_3\dot{\text{C}}\text{H}_2$  adduct of DBNBS and the fourth adduct (lines marked D) obtained in the sonolysis of  $\text{CH}_3\text{CH}_2\text{OH}-\text{H}_2\text{O}$  (5%) was found to be the same. Hence, the ESR spectrum of the fourth spin adduct (lines marked D) has been assigned to the  $\text{CH}_3\dot{\text{C}}\text{H}_2$  radical. Additional support for this assignment has been obtained from

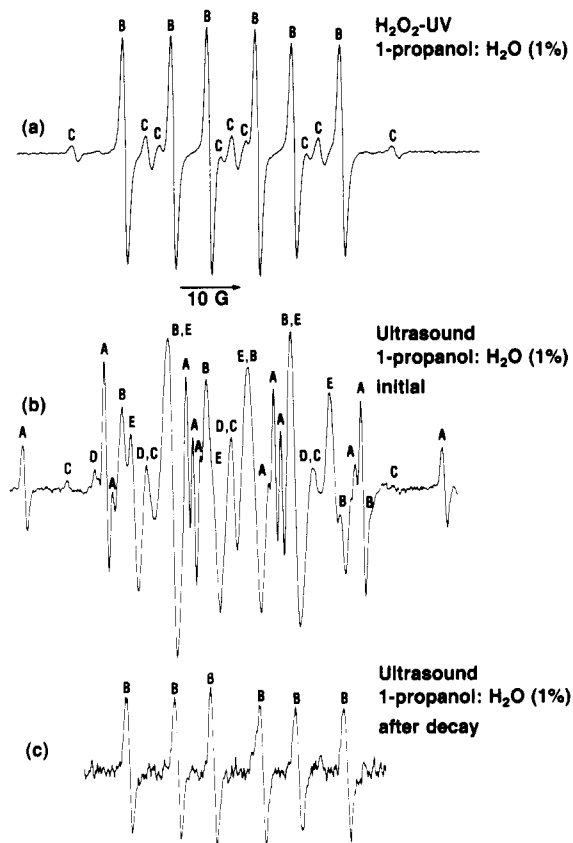


**Figure 3.** ESR spectra of spin adducts obtained from  $\text{CH}_3(\text{CH}_2)_2\text{OH}-\text{H}_2\text{O}$  (1:99, v/v): (a) sample in the presence of  $\text{H}_2\text{O}_2$  (2 mM) and DBNBS (3 mM) after 2-min exposure to 275-nm light; (b) sonolysis (10 min) or argon-saturated solutions in the presence of DBNBS (3 mM), recorded immediately after sonication; (c) same conditions as (b), recorded 2 h after sonication.

the sonolysis of  $\text{CH}_3\text{CD}_2\text{OH}-\text{H}_2\text{O}$  (5%), the ESR spectrum of which did not exhibit ESR lines at the field positions expected for the  $\text{CH}_3\dot{\text{C}}\text{H}_2$  adduct.

In order to study the origin of methyl adducts of DBNBS from ethanol, mixed-isotope systems such as  $\text{CH}_3\text{CD}_2\text{OH}-\text{H}_2\text{O}$  and  $\text{CD}_3\text{CH}_2\text{OH}-\text{H}_2\text{O}$  have been studied by spin trapping. Traces a and b of Figure 2 show the ESR spectra obtained by sonication of argon-saturated  $\text{CH}_3\text{CD}_2\text{OH}-\text{H}_2\text{O}$  (5:95) and  $\text{CD}_3\text{CH}_2\text{OH}-\text{H}_2\text{O}$  (5:95), respectively, in the presence of DBNBS. The ESR spectrum in Figure 2a obtained by sonolysis of argon-saturated  $\text{CH}_3\text{CD}_2\text{OH}-\text{H}_2\text{O}$  (5%) indicates that the isotopic composition of the methyl radicals is predominantly  $\dot{\text{C}}\text{H}_3$ , suggesting that methyl radicals are formed by the C–C scission of the ethanol molecule. However, the presence of small quantities of isotopically mixed methyl radicals,  $\dot{\text{C}}\text{H}_2\text{D}$  and  $\dot{\text{C}}\text{H}_2\text{D}_2$ , indicates that a small part of the methyl radical yield could result from reactions mediated by radical recombinations prior to the C–C scission. These observations have been complemented by sonolysis experiments with  $\text{CD}_3\text{CH}_2\text{OH}-\text{H}_2\text{O}$  (5:95) where  $\dot{\text{C}}\text{D}_3$  was the major product with small yields of  $\dot{\text{C}}\text{D}_2\text{H}$  radicals (Figure 2b). Further support for this observation has been obtained by sonolysis experiments with  $^{12}\text{CH}_3^{13}\text{CH}_2\text{OH}-\text{H}_2\text{O}$  (5:95) in the presence of DBNBS in which only  $^{12}\text{C}\dot{\text{H}}_3$  radicals were detected.

**1-Propanol.**  $\text{H}_2\text{O}_2$ -UV photolysis of argon-saturated 1-propanol– $\text{H}_2\text{O}$  (1%) in the presence of DBNBS resulted in the observation of two different spin adducts (Figure 3a). The first spin adduct exhibited an ESR spectrum with a primary nitrogen splitting of 14.38 G and a secondary 1:2:1 triplet due to two equivalent protons ( $a_{2\text{H}} = 12.25$  G). These splittings are consistent with a  $\dot{\text{C}}\text{H}_2\text{CH}_2\text{CH}_2\text{OH}$  adduct of DBNBS produced by H abstraction from the methyl group of 1-propanol. The second spin adduct from 1-propanol exhibited an ESR spectrum with a primary nitrogen splitting ( $a_{\text{N}} = 13.25$  G); each line of the triplet is further split into a secondary doublet by a proton ( $a_{\text{H}} = 8.00$

G). The structure of this radical could be either  $\text{CH}_3\text{CH}_2\dot{\text{C}}\text{HOH}$  or  $\text{CH}_3\dot{\text{C}}\text{HCH}_2\text{OH}$ . However, it was not possible to distinguish between these two possibilities. Identical spin adducts were obtained by  $\gamma$ -radiolysis of  $\text{N}_2\text{O}$ -saturated solutions of 1-propanol- $\text{H}_2\text{O}$  (5:95).

Sonolysis of argon-saturated 1-propanol- $\text{H}_2\text{O}$  (1%) in the presence of DNBNS resulted in the formation of five different spin adducts (Figure 3b). The first spin adduct (lines marked A) has been identified as a  $\dot{\text{C}}\text{H}_3$  adduct of DNBNS based on the ESR parameters. The ESR spectrum of the second spin adduct (lines marked B) obtained by sonolysis of 1-propanol- $\text{H}_2\text{O}$  (1%) was found to exhibit a primary nitrogen-split triplet ( $a_{\text{N}} = 14.0$  G) further split into a secondary doublet by a proton ( $a_{\text{H}} = 8.0$  G). This adduct is similar to one of the adducts (lines marked B, Figure 3a) obtained by  $\text{H}_2\text{O}_2$ -UV photolysis or  $\gamma$ -radiolysis of 1-propanol- $\text{H}_2\text{O}$  solutions. The structure of this radical has been assigned to  $\dot{\text{C}}\text{H}_3\dot{\text{C}}\text{HCH}_2\text{OH}$  or  $\text{CH}_3\text{CH}_2\dot{\text{C}}\text{HOH}$ . The third spin adduct observed in the sonolysis of 1-propanol- $\text{H}_2\text{O}$  (1%) exhibited weak ESR lines (marked C). Only the ESR lines at the low-field and the high-field positions could be identified because of the large overlap due to the ESR lines from spin adducts formed in relatively larger quantities. The field separation of these lines was found to be 53.25 G, indicating that this spin adduct is of the  $\dot{\text{C}}\text{H}_2$  type. The field separation for this adduct agrees well with that of the  $\dot{\text{C}}\text{H}_2\text{CH}_2\text{CH}_2\text{OH}$  obtained by  $\text{H}_2\text{O}_2$ -UV photolysis and  $\gamma$ -radiolysis of aqueous 1-propanol solutions, indicating that the third spin adduct (lines marked C) obtained by sonolysis of aqueous 1-propanol is  $\dot{\text{C}}\text{H}_2\text{CH}_2\text{CH}_2\text{OH}$ .

Another  $\dot{\text{C}}\text{H}$  radical adduct with small yields (lines marked E) is obtained in the sonolysis of 1-propanol- $\text{H}_2\text{O}$  (1%). All of the ESR lines of this spin adduct could not be marked due to overlapping ESR lines from other spin adducts formed in larger quantities. The approximate hyperfine coupling constants of this  $\dot{\text{C}}\text{H}$  adduct are  $a_{\text{N}} = 14.0$  G and  $a_{\text{H}} = 6.25$  G. It was not possible to obtain additional information about the identity of this radical adduct.

Indications of the presence of a fifth adduct was found (lines marked D, Figure 3b). On the basis of the field positions of the ESR lines of this adduct, the radical could be a  $\dot{\text{C}}\text{H}_2$ -type adduct. However, the low yields of formation of this adduct and the large overlap of these weak lines by intense ESR lines of the other spin adducts did not permit the characterization of this spin adduct.

**2-Propanol.**  $\text{H}_2\text{O}_2$ -UV photolysis of 2-propanol- $\text{H}_2\text{O}$  (1%) in the presence of DNBNS resulted in the observation of one spin adduct, the ESR spectrum of which (Figure 4a) exhibits a primary nitrogen-split triplet ( $a_{\text{N}} = 14.0$  G) further split into twelve lines due to two inequivalent protons ( $a_{\text{H1}} = 11.5$  G;  $a_{\text{H2}} = 9.63$  G). Each of these twelve lines is further split into a doublet due to a  $\gamma$ -proton ( $a_{\gamma\text{H}} = 0.5$  G) (seen only under low modulation and power). On the basis of these ESR parameters, this spin adduct has been assigned as due to the  $\text{CH}_3\dot{\text{C}}\text{HOHCH}_2$  radical. A similar spin adduct has been obtained in the  $\gamma$ -radiolysis of  $\text{N}_2\text{O}$ -saturated solutions of 2-propanol in the presence of DNBNS. The splitting constants observed for this adduct are very close to those reported previously for this radical by Kaur et al.<sup>12a</sup> in which this radical was generated by  $\text{H}_2\text{O}_2$ -UV photolysis of 2-propanol solutions. However, in another study,<sup>12c</sup> the splitting constants reported for this adduct are different ( $a_{\text{H1}} = a_{\text{H2}} = 10.6$  G). This difference could be attributed to different solvent compositions. Another radical,  $(\text{CH}_3)_2\dot{\text{C}}\text{OH}$ , known to be formed in OH radical reactions with 2-propanol, is not trapped in the present study, in agreement with previous reports,<sup>12</sup> presumably due to steric hindrance to trapping.

Sonolysis of argon-saturated 2-propanol- $\text{H}_2\text{O}$  (1%) resulted in the detection of three different spin adducts (Figure 4b). The first spin adduct (lines marked A) has been interpreted as due to the  $\dot{\text{C}}\text{H}_3$  radical based on its characteristic ESR spectrum. The second spin adduct (lines marked B), which is formed in relatively small yields, is analyzed as due to the  $\text{CH}_3\dot{\text{C}}\text{HOHCH}_2$  radical based on its ESR spectrum ( $a_{\text{N}} = 14.0$  G;  $a_{\text{H1}} = 11.5$  G;  $a_{\text{H2}} = 9.63$  G;  $a_{\gamma\text{H}} = 0.5$  G). This radical has been trapped in the  $\text{H}_2\text{O}_2$  UV photolysis and the  $\gamma$ -radiolysis of 2-propanol solutions. The

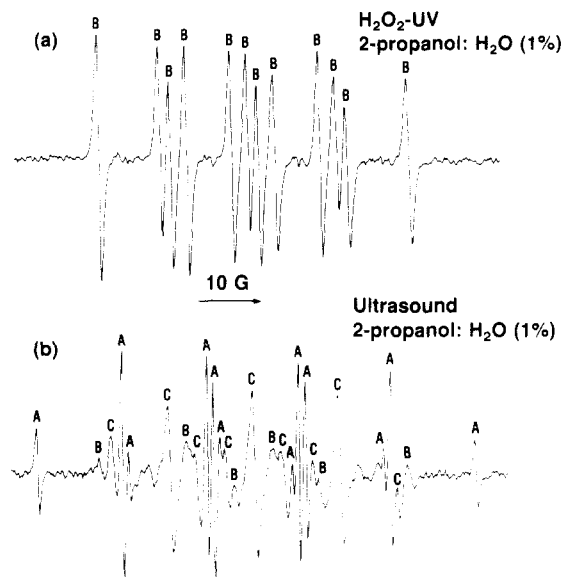


**Figure 4.** ESR spectra of spin adducts obtained from  $(\text{CH}_3)_2\text{CHOH}-\text{H}_2\text{O}$  (1:99, v/v): (a) sample in the presence of  $\text{H}_2\text{O}_2$  (2 mM) and DNBNS (3 mM) after 2-min exposure to 275-nm light; (b) sonolysis (10 min) of argon-saturated solutions in the presence of DNBNS (3 mM), recorded immediately after sonication.

ESR spectrum of the third spin adduct (lines marked C, Figure 4b) has been analyzed as due to a primary nitrogen triplet ( $a_{\text{N}} = 13.5$  G) further split into a secondary 1:2:1 triplet due to two equivalent protons ( $a_{2\text{H}} = 9.25$  G). The ESR parameters of this spin adduct have been found to be similar to the acetyl radical  $\dot{\text{C}}\text{H}_2\text{COCH}_3$  adduct of DNBNS generated by  $\text{H}_2\text{O}_2$ -UV photolysis of acetone (1%). Hence, this spin adduct (lines marked C, Figure 4b) has been assigned to the  $\dot{\text{C}}\text{H}_2\text{COCH}_3$  adduct of DNBNS in the sonolysis of 2-propanol (1%). The precursor of this radical, acetone, is presumably formed by disproportionation of two  $(\text{CH}_3)_2\dot{\text{C}}\text{OH}$  radicals.

**2-Methyl-2-propanol.**  $\text{H}_2\text{O}_2$ -UV photolysis of 2-methyl-2-propanol- $\text{H}_2\text{O}$  (1%) in the presence of DNBNS resulted in the observation of a single spin adduct (Figure 5a) whose ESR spectrum exhibited a primary nitrogen-split triplet ( $a_{\text{N}} = 13.5$  G) and a secondary 1:2:1 triplet due to equivalent protons ( $a_{2\text{H}} = 9.63$  G). On this basis of its ESR parameters, this adduct has been identified as due to the  $(\dot{\text{C}}\text{H}_2)(\text{CH}_3)_2\text{COH}$  adduct of DNBNS. A similar spin adduct has been observed in the  $\gamma$ -radiolysis of 2-methyl-2-propanol- $\text{H}_2\text{O}$  (1%).

Argon-saturated 2-methyl-2-propanol- $\text{H}_2\text{O}$  (1%) yielded three different spin adducts after sonication in the presence of DNBNS (Figure 5b). The first spin adduct (lines marked A, Figure 5b) is a typical  $\dot{\text{C}}\text{H}_3$  adduct exhibiting its characteristic ESR spectrum. The second spin adduct (lines marked B, Figure 5b) exhibits a primary nitrogen triplet ( $a_{\text{N}} = 13.5$  G) further split into a 1:2:1 triplet ( $a_{2\text{H}} = 9.6$  G) due to two equivalent protons. This spectrum is identical with that obtained in the  $\text{H}_2\text{O}_2$ -UV photolysis (Figure 5a) and that observed in the  $\gamma$ -radiolysis of 2-methyl-2-propanol- $\text{H}_2\text{O}$  (1%) and is identified as due to the  $(\dot{\text{C}}\text{H}_2)-(\text{CH}_3)_2\text{COH}$  radical. When the ESR spectrum is recorded at various times after sonolysis, it was noted that the ESR lines due to the  $\dot{\text{C}}\text{H}_3$  adduct and the  $(\dot{\text{C}}\text{H}_2)(\text{CH}_3)_2\text{COH}$  adduct decay and a three-lined ESR spectrum becomes predominant (lines marked C, Figure 5c) with no lines due to secondary hyperfine splittings, indicating that this adduct could be due to the  $(\text{CH}_3)_3\dot{\text{C}}$  radical.

#### Isotope-Exchange Reactions

Henglein and his co-workers studied sonochemical effects on mixed-isotope systems<sup>4,15</sup> and proposed successive radical-recom-

(15) (a) Fischer, Ch.-H.; Hart, E. J.; Henglein, A. *J. Phys. Chem.* **1986**, *90*, 3959. (b) Fischer, Ch.-H.; Hart, E. J.; Henglein, A. *J. Phys. Chem.* **1986**, *90*, 1954. (c) Hart, E. J.; Fischer, Ch.-H.; Henglein, A. *J. Phys. Chem.* **1986**, *90*, 5989.

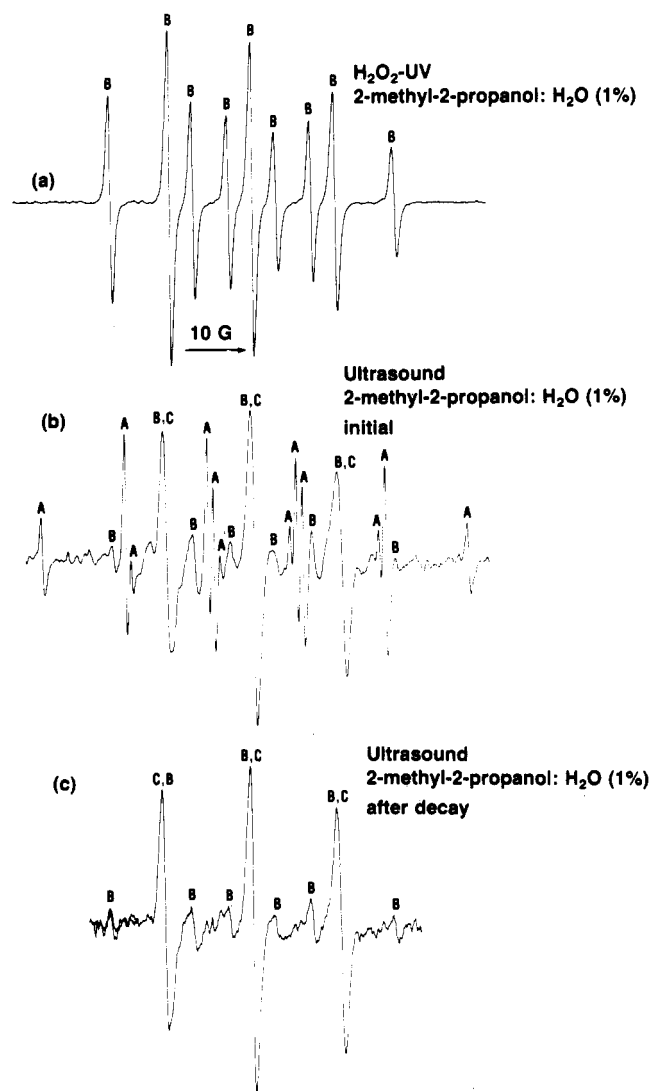


**Figure 5.** ESR spectra of spin adducts obtained from  $(\text{CH}_3)_3\text{COH}:\text{H}_2\text{O}$  (1:99, v/v): (a) sample in the presence of  $\text{H}_2\text{O}_2$  (2 mM) and DBNBS (3 mM) after 2-min exposure to 275-nm light; (b) sonolysis (10 min) of argon-saturated solutions in the presence of DBNBS (3 mM), recorded immediately after sonication; (c) same conditions as (b), recorded 2 h after sonication.

**TABLE II: Ratio of ESR Signal Intensities of the DBNBS Adducts of  $\dot{\text{C}}\text{H}_2\text{D}$  and  $\dot{\text{C}}\text{H}_3$  Radicals Obtained by Sonolysis of Mixed-Isotope Systems of Various Water–Alcohol Mixtures**

system	$\dot{\text{C}}\text{H}_2\text{D}/\dot{\text{C}}\text{H}_3^a$
$\text{CH}_3\text{OD}-\text{D}_2\text{O}$ (5%)	0.63
$\text{CH}_3\text{CH}_2\text{OD}-\text{D}_2\text{O}$ (1%)	0.49
$\text{CH}_3\text{CD}_2\text{OH}-\text{H}_2\text{O}$ (1%)	0.20
$\text{CH}_3\text{CD}_2\text{OD}-\text{D}_2\text{O}$ (1%)	0.53
$\text{CH}_3(\text{CH}_2)_2\text{OD}-\text{H}_2\text{O}$ (1%)	0.35
$(\text{CH}_3)_2\text{CHOD}-\text{H}_2\text{O}$ (1%)	0.24
$(\text{CH}_3)_3\text{COD}-\text{H}_2\text{O}$ (1%)	0.16

<sup>a</sup> The ESR spectra of the DBNBS adducts of  $\dot{\text{C}}\text{H}_3$  and  $\dot{\text{C}}\text{H}_2\text{D}$  have been corrected for their different multiplicities to calculate the ratio of their relative concentrations.

bination reactions to occur in the gas bubbles in order to explain the isotopically scrambled products detected. Isotopically mixed products of methyl radicals ( $\dot{\text{C}}\text{H}_2\text{D}$ ) have also been detected in the present study in the sonolysis of alcohol–water mixtures of the type  $\text{ROD}-\text{D}_2\text{O}$ . Similar products ( $\dot{\text{C}}\text{H}_2\text{D}$ ) were also detected in the sonolysis of  $\text{CH}_3\text{CD}_2\text{OH}-\text{H}_2\text{O}$  and  $\text{CD}_3\text{CH}_2\text{OH}-\text{H}_2\text{O}$  (Figure 2). ESR lines characteristic of the  $\dot{\text{C}}\text{H}_2\text{D}$  adduct of DBNBS- $d_2$  have been identified in the sonolysis of various  $\text{ROD}-\text{D}_2\text{O}$  mixtures, and the yield of this adduct was compared with that of the  $\dot{\text{C}}\text{H}_3$  adduct after normalizing for their differing

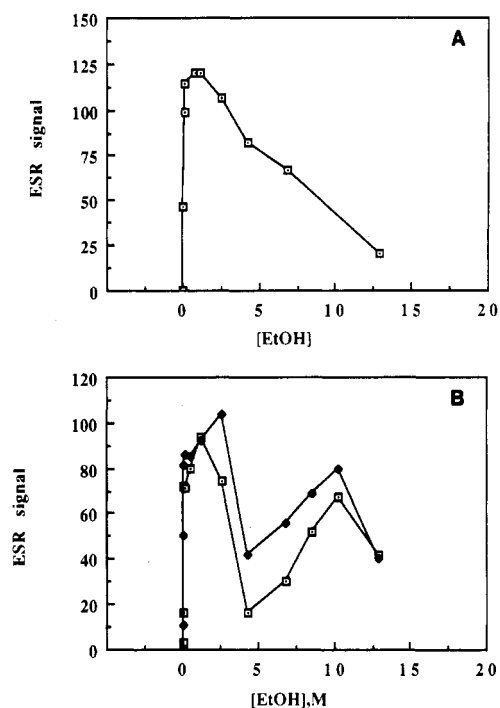
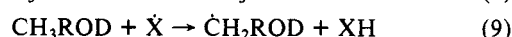
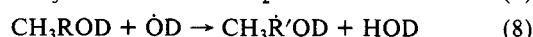
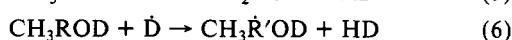
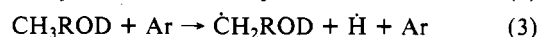
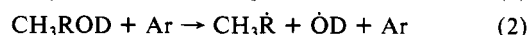
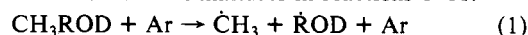


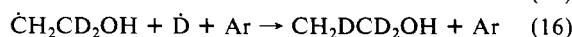
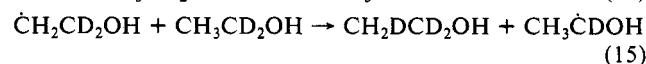
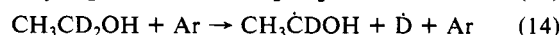
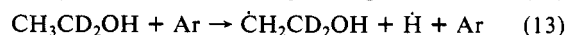
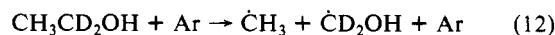
**Figure 6.** (A) ESR signal intensity (arbitrary units) of DBNBS- $\text{CH}_2\text{-CH}_2\text{OH}$  obtained by 275-nm illumination (90 s) in the presence of  $\text{H}_2\text{O}_2$  (2 mM) and DBNBS (3 mM) plotted as a function of ethanol concentration. (B) ESR signal intensity (arbitrary units) of DBNBS- $\text{CH}_3$  adduct ( $\square$ ) and DBNBS- $\text{CH}_2\text{CH}_2\text{OH}$  adduct ( $\blacklozenge$ ) obtained by sonolysis (10 min) of argon-saturated  $\text{CH}_3\text{CH}_2\text{OH}-\text{H}_2\text{O}$  mixtures in the presence of DBNBS (3 mM) plotted as a function of ethanol concentration.

multiplicities. The results are presented in Table II. A reaction scheme involving multiple radical reactions has been proposed<sup>11</sup> to explain the sonochemically induced formation of  $\dot{\text{C}}\text{H}_2\text{D}$  radicals from the  $\text{CH}_3\text{OD}-\text{D}_2\text{O}$  mixtures. This scheme can be generalized for the various water–alcohol mixtures in reactions 1–11.



X is any of the radicals D, OD,  $\text{CH}_3$ , H, etc.

The formation of  $\dot{\text{C}}\text{H}_2\text{D}$  radicals during the sonolysis of  $\text{CH}_3\text{CD}_2\text{OH}-\text{H}_2\text{O}$  can also be explained in terms of multiple radical reactions in the cavitation gas bubbles. Following thermal decomposition of  $\text{CH}_3\text{CD}_2\text{OH}$  to give  $\dot{\text{C}}\text{H}_2\text{CD}_2\text{OH}$ , reaction of this radical with ethanol will give  $\text{CH}_2\text{DCD}_2\text{OH}$ , which after subsequent pyrolysis gives the  $\dot{\text{C}}\text{H}_2\text{D}$  adduct as described in eq 12–17.



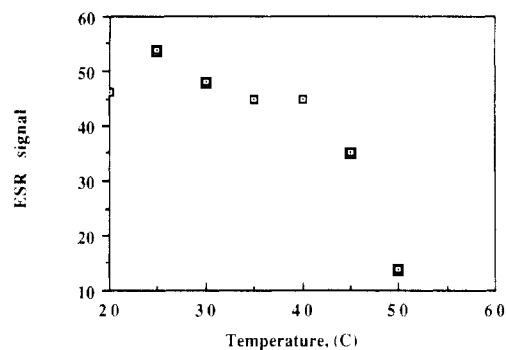


**Figure 7.** ESR signal intensity (arbitrary units) of DNBBS- $\dot{\text{C}}\text{H}_3$  adduct obtained by sonolysis (10 min) at different sample temperatures of argon-saturated  $\text{CH}_3\text{CH}_2\text{OH}-\text{H}_2\text{O}$  (10:90, v/v), in the presence of DNBBS (3 mM).

The possibility of an intramolecular deuterium 1,2-transfer<sup>16</sup> in  $\dot{\text{C}}\text{H}_2\text{CD}_2\text{OH}$  to give  $\text{CH}_2\text{D}\dot{\text{C}}\text{DOH}$  cannot be ruled out.

### Effect of Solvent Composition on Spin Adduct Yields

In order to study the effect of solvent composition of water-alcohol mixtures on the spin adduct yields obtained by sonolysis, the water-ethanol system was chosen because of the simplicity of the total ESR spectrum obtained by sonolysis. Furthermore, the spin trap DNBBS is soluble at the optimum concentration over the entire range of the solvent compositions studied. However, prior information about the spin-trapping efficiency of DNBBS under varying solvent compositions is needed to make a proper analysis of the sonochemically induced spin adduct yields in the same range of solvent compositions. Figure 6a shows the yield of the  $\dot{\text{C}}\text{H}_2\text{CH}_2\text{OH}$  adduct of DNBBS formed after 90-s exposure to 275-nm light in the presence of  $\text{H}_2\text{O}_2$  (2 mM) and DNBBS (3 mM) in various water-ethanol mixtures, all other experimental conditions being identical. The yield of DNBBS- $\dot{\text{C}}\text{H}_2\text{CH}_2\text{OH}$  was found to increase with increasing ethanol concentrations and reached a maximum at 3 M ethanol. The decrease above 3 M can be understood in terms of a competition for the  $\dot{\text{C}}\text{H}_2\text{CH}_2\text{OH}$  radical between DNBBS and  $\text{CH}_3\text{CH}_2\text{OH}$ . The latter reaction leads to the formation of  $\text{CH}_3\dot{\text{C}}\text{HOH}$ ,<sup>17</sup> the spin adduct of which, as discussed in an earlier section, is not observed with DNBBS in a steady-state reaction system.

Figure 6b shows the yield of the DNBBS adducts of  $\dot{\text{C}}\text{H}_3$  and  $\dot{\text{C}}\text{H}_2\text{CH}_2\text{OH}$  obtained by sonolysis at different compositions of water-ethanol mixtures. The other spin adducts obtained by sonolysis of aqueous ethanol, namely, those of the  $\dot{\text{C}}\text{H}_2\text{CHO}$  and the  $\text{CH}_3\dot{\text{C}}\text{H}_2$  radicals, are not shown in this plot because of large overlap with ESR lines of other spin adducts formed in higher yields, thereby preventing a reliable quantitative estimate. Two maxima were found for the two spin adducts plotted, in the range of the solvent compositions studied. The initial maximum for the  $\dot{\text{C}}\text{H}_3$  adduct was observed at  $\approx 2$  M and that for the  $\dot{\text{C}}\text{H}_2\text{CH}_2\text{OH}$  at  $\approx 3$  M, which is in the same region as that observed in Figure 6a. This result has been confirmed by repeating the experiment five times. The initial maximum for the  $\dot{\text{C}}\text{H}_3$  and the  $\dot{\text{C}}\text{H}_2\text{CH}_2\text{OH}$  adducts in Figure 6b can be attributed to the changes of spin-trapping efficiency at different solvent compositions. The different values of the initial maxima of the  $\dot{\text{C}}\text{H}_3$  and the  $\dot{\text{C}}\text{H}_2\text{CH}_2\text{OH}$  adducts can be attributed to the different reactivities of the  $\dot{\text{C}}\text{H}_3$  and the  $\dot{\text{C}}\text{H}_2\text{CH}_2\text{OH}$  radicals with  $\text{CH}_3\text{CH}_2\text{OH}$  to form  $\text{CH}_3\dot{\text{C}}\text{HOH}$  radicals.<sup>18</sup> The second maximum of the  $\dot{\text{C}}\text{H}_3$  and the  $\dot{\text{C}}\text{H}_2\text{CH}_2\text{OH}$  adducts ( $\approx 10$  M) occurs in a region where an

apparent decrease in the spin adduct yield is expected with increasing ethanol concentration, based on the spin-trapping efficiency (Figure 6a). This observation indicates that the second maximum of the yield of the spin adducts observed in the sonolysis of ethanol is due to acoustic cavitation. The two maxima of the spin adduct yields in the range of solvent compositions of the ethanol-water mixtures investigated can be understood in terms of a superposition of the maximum due to the spin-trapping efficiency and the maximum due to the sonochemical yield. The observation of two maxima of spin adduct yields in the sonolysis of water-ethanol mixtures is in contrast to the results obtained in water-methanol mixtures, where only a single maximum of the  $\dot{\text{C}}\text{H}_3$  adduct yield was observed at 5 M.<sup>11</sup> This result could be understood in terms of an overlap of the maximum due to spin-trapping efficiency and the maximum due to acoustic cavitation.

Numerous factors influence the acoustic cavitation and the sonochemical yields.<sup>19</sup> In the bulk solution, factors favoring maximum acoustic cavitation are (i) low viscosity, (ii) high surface tension, (iii) low vapor pressure, and (iv) high sound speed. In the gas phase, acoustic cavitation is enhanced when the gas contents of the cavitating bubbles have a high  $C_p/C_v$  and low thermal conductivity (since the cavitation collapse is not completely adiabatic), thus increasing the final collapse temperature. At 25 °C, the surface tension of ethanol-water mixtures decreases slightly with increasing ethanol content.<sup>20</sup> The viscosity of various water-ethanol mixtures was measured at 25 °C and was found to increase with increasing ethanol concentrations from 1.25 cP at 1 M to a maximum of 2.5 cP at 9 M ethanol. The vapor pressure of water-ethanol mixtures increases with increasing ethanol content. Hence, it is difficult to correlate the second maximum observed at 10 M in Figure 6b with a single factor influencing acoustic cavitation.

Suslick et al.<sup>21</sup> have demonstrated that the vapor pressure of the bulk liquid is the major factor influencing the cavitation efficiency in organic liquids and hence the sonochemical rates. In order to study the role of vapor pressure on sonochemical yields, spin-trapping experiments were carried out with  $\text{CH}_3\text{CH}_2\text{OH}-\text{H}_2\text{O}$  (10%) and DNBBS (3 mM) and the mixtures were sonicated at different temperatures under identical experimental conditions. Increasing the temperature causes an increase in vapor pressure and a decrease in viscosity. The yield of the methyl radical adduct of DNBBS obtained by sonolysis of  $\text{CH}_3\text{CH}_2\text{OH}-\text{H}_2\text{O}$  (10%) as a function of bulk solution temperature (20–50 °C) is shown in Figure 7. The spin adduct yield was observed to slightly increase with increasing temperature from 20 to 25 °C and decrease markedly in the region from 25 to 50 °C. This result is in agreement with the work of Suslick et al.<sup>20</sup> where the sonochemical rates have been studied as a function of solvent vapor pressure and the log of the sonochemical rate was found to decrease with increasing solvent vapor pressure.

A more complete understanding of the sonochemistry of aqueous alcohol mixtures requires the identification of the stable sonoproducts and their variation as a function of solvent composition.

**Registry No.** DNBBS- $d_2/\dot{\text{C}}\text{H}_3$  spin adduct, 78824-00-7; DNBBS- $d_2/\dot{\text{C}}\text{H}_2\text{CH}_2\text{OH}$  spin adduct, 78824-02-9; DNBBS- $d_2/\dot{\text{C}}\text{H}_2\text{CHO}$  spin adduct, 120789-08-4; DNBBS- $d_2/\dot{\text{C}}\text{H}_3\text{CH}_2$  spin adduct, 120789-09-5; DNBBS- $d_2/\dot{\text{C}}\text{H}_3\text{CHCH}_2\text{OH}$  spin adduct, 120789-10-8; DNBBS- $d_2/\dot{\text{C}}\text{H}_3\text{CH}(\text{OH})\dot{\text{C}}\text{H}_2$  spin adduct, 78824-08-5; DNBBS- $d_2/\dot{\text{C}}\text{H}_2\text{COCH}_3$  spin adduct, 120789-11-9; DNBBS- $d_2/(\dot{\text{C}}\text{H}_2)(\text{CH}_3)_2\text{COH}$  spin adduct, 120789-12-0; DNBBS- $d_2/\dot{\text{C}}(\text{CH}_3)_3$  spin adduct, 78824-07-4; DNBBS- $d_2\text{-Na}$ , 78824-11-0;  $\text{CH}_3\text{CH}_2\text{OH}$ , 64-17-5;  $\text{CH}_3(\text{CH}_2)_2\text{OH}$ , 71-23-8;  $(\text{CH}_3)_2\text{CHOH}$ , 67-63-0;  $(\text{CH}_3)_3\text{COH}$ , 75-65-0;  $\text{H}_2\text{O}_2$ , 7722-84-1;  $\text{I}(\text{C}-\text{H}_2)_2\text{OH}$ , 624-76-0;  $\text{CH}_3\text{CHO}$ , 75-07-0;  $\text{C}_2\text{H}_5\text{I}$ , 75-03-6;  $\text{H}_2$ , 1333-74-0; acetone, 67-64-1.

(16) (a) Gordon, A. S.; Tardy, D. C.; Ireton, R. J. *Phys. Chem.* **1976**, *80*, 1400. (b) Dobe, S.; Berces, T. In *Chemical Kinetics of Small Organic Radicals*; Alfassi, Z. B., Ed.; CRC Press: Boca Raton, FL, 1988; Vol. 1, p 95.

(17) Burchill, C. E.; Ginns, I. S. *Can. J. Chem.* **1970**, *48*, 2628.

(18) Ross, A.; Neta, P. *Natl. Stand. Ref. Data Ser. (U.S., Natl. Bur. Stand.)* **1982**, NSRDS-NBS-70.

(19) Flynn, H. G. In *Physical Acoustics: Principles and Methods*; Mason, W. P., Ed.; Academic Press: New York, 1964; p 165.

(20) *International Critical Tables*; McGraw-Hill: New York, 1928; Vol. III, p 467.

(21) Suslick, K. S.; Gawienowski, J. J.; Schubert, P. F.; Wang, H. H. *Ultrasonics* **1984**, *22*, 33.